

Two-Beam Coupling Correlation Synthetic Aperture Radar Image Recognition with Power-law Scattering Centers pre-enhancement

Bahareh Haji-saeed¹, Jed Khoury², Charles L. Woods² and John Kierstead¹

¹ Solid State Scientific Corporation, Hollis, NH 03049

² Air Force Research Laboratory / SNHC, Hanscom Air Force Base, MA 01731

ABSTRACT

Synthetic radar image recognition is an area of interest for military applications including automatic target recognition, air traffic control, and remote sensing. Here a dynamic range compression two-beam coupling joint transform correlator for detecting synthetic aperture radar (SAR) targets is utilized. The joint input image consists of a pre-power-law, enhanced scattering center of the input image and a linearly synthesized power-law enhanced scattering center template. Enhancing the scattering center of both the synthetic template and the input image furnishes the conditions for achieving dynamic range compression correlation in two-beam coupling. Dynamic range compression: (a) enhances the signal to noise ratio, (b) enhances the high frequencies relative to low frequencies, and (c) converts the noise to high frequency components. This improves the correlation peak intensity to the mean of the surrounding noise significantly. Dynamic range compression correlation has already been demonstrated to outperform many optimal correlation filters in detecting signals in severe noise environments. The performance is evaluated via established metrics, such as peak-to-correlation energy (PCE), Horner efficiency and correlation peak intensity. The results showed significant improvement as the power increased.

Keywords: Pattern recognition, correlation, synthetic aperture radar (SAR)

1. INTRODUCTION

Synthetic radar image recognition and classification are areas of interest for both the military and civilian communities. These tasks have significance in automatic target recognition, air traffic control, and remote sensing. Equivalent problems of recognition and classification are also of interest for the ultrasonic and sonar images communities, for which numerous algorithms such as neural networks¹, wavelets², fuzzy logic³, mean-square error-matching templates⁴ and feature base classifications⁵ have been used. Although the processors involved in these techniques are claimed to be real-time, they require an extensive amount of time for calculations, making it very difficult to track targets with them in real time. Moreover, these techniques require a digital workstation for data processing in real time. Furthermore, SAR image information is blurred by the radar ambiguity function,^{6,7} which relates the uncertainty between the target range and its range rate. Unfortunately, accuracy in the measurement of one of these quantities usually comes at the expense of the other. Although the role of the ambiguity function in image blurring is similar to that of the point-spread function in optical imaging, its effect is much more severe. The above facts make it hard to recognize SAR images compared to optical images which have resolution within a few micrometers. SAR images are dominated by a few strong scattering centers. These scattering centers play the role as the finger prints identification of SAR images.

In our prior work, a new correlation technique for recognition of targets from Moving and Stationary Target Acquisitions (MSTAR) Database^{8,9} was introduced. In this technique a modified version of the phase-only filter and the binary phase-only filter algorithms was used^{10,11}. In advance to performing the correlation, both the input and the matching template scattering centers were pre-enhanced via the power-law enhancement processing on both the template and the input. The matching template filter was made from enhanced scattering centers of images' region of interest (ROI). We have also introduced a new category of companding nonlinear processors for noise reduction¹², correlators¹³⁻¹⁶, and image restoration¹⁷⁻¹⁹ based on companding coupling in nonlinear holographic media. The companding correlators showed a significant improvement on both phase and binary phase only filters in detection of signals embedded in a very high noise environment. The dynamic range compression associated with these correlators works on noise reduction as well as enhancement of the correlation peak to its surrounding noise.

In this paper, we extended our work by combining the two prior techniques (i.e. the power-law scattering centers enhancement and two-beam coupling dynamic range compression) for SAR image recognition. The power-law enhancements of the scattering centers facilitate the necessary preconditions: (a) for less severe requirements to achieve dynamic range compression, and (b) for blocking the noise with a small loss in the scattering centers spectrum. Casasent's and his co-workers demonstrated correlation based on optimized synthetic discriminant functions (SDF), however they did not do any scattering centers enhancements for their identification approach^{20, 21}.

2. DYNAMIC RANGE COMPRESSION

Dynamic Range Compression/Expansion known as companding (compressing-expanding) is a well-established principle for recovering signals embedded in high noise. Dynamic Range Compression/Expansion nonlinearity²²⁻²⁵, when it is applied to a noisy signal, improves the signal to noise ratio in areas where the signal is low compared to the noise and reduces the SNR in areas where the signal is higher than the noise level. This principle has been used for improving the quality of acoustic signals in the 50's and is extensively used for noise reduction in tape recording which is limited by "tape hiss", which is high frequency random noise. Noise reduction systems like the "Dolby" and "dbx" help to solve this problem by pre-emphasizing (compression) the high frequencies before recording onto tape in order to make them higher in amplitude than the tape hiss noise with which they compete and then upon playback, a matched de-emphasis filter (expansion) is employed. In Fourier processing, applying dynamic range compression: (1) enhances the signal to noise ratio where the SNR is low, (2) increases the noise frequency which leads to spreading the noise over a larger area in the other domain, which consequently has a significant affect on SNR enhancement in the image plane., and (3) enhances the high frequencies relative to the low frequencies. This is an essential functionality for the recovery of high frequencies intensity in blurred signals, or for enhancing the high frequencies relative to low frequencies for increasing the discrimination capability of pattern recognition. These three advantages of applying dynamic range compression on noisy signals in spectral domain lead to significant improvement of processed data relative to noise. We have already demonstrated the enhancement in both of companding optical correlators¹³⁻¹⁶ and compression deconvolution processors¹⁷⁻¹⁹.

3. TWO-BEAM COUPLING- JOINT FOURIER PROCESSOR

Photorefractive two-beam coupling joint Fourier processor already has been discussed in several references. Figure 1 shows the architecture of a two-beam coupling joint Fourier processor.

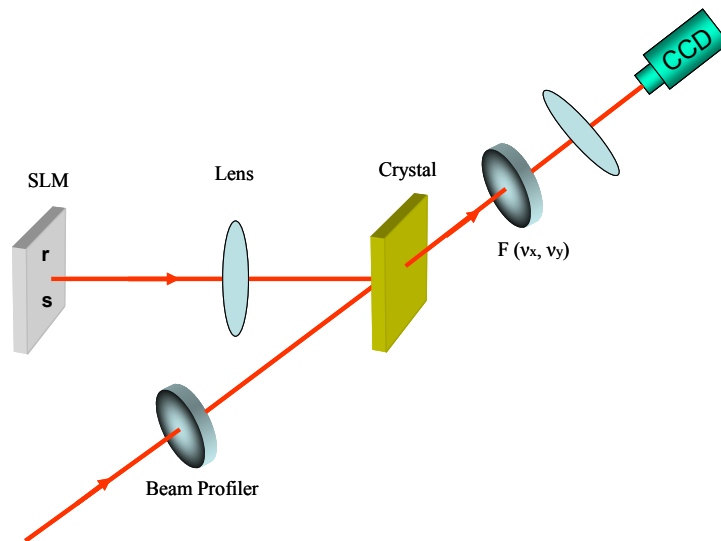


Figure 1. Two beam-coupling joint Fourier processor.

A signal beam passes through the SLM which is addressed by a joint image of signal and reference information. The joint image then is Fourier transformed via a lens to pump a spectrally variant reference beam. The reference beam is shaped through a beam profiler. A beam profiler is a SLM addressed either by an expected spectrum of the joint spectrum or adaptively addressed by the joint spectra envelope through direct measurement. The beam profiler is essential for reducing the extremely high beam ratios constrain required to achieve dynamic range compression. The deflected output from the crystal is Fourier transformed to produce the joint spectra processed image.

In the diffusion limit with no absorption, when a clean beam with spatially variant amplitude, $A(0)/I(0)$, pumps a beam bearing the joint spectra of two images r and s , the output at the crystal (Fourier) plane can be written as:

$$A(v_x, v_y) = A(0) \left[\frac{1 + m/(\lambda f_l)^2 |R(v_x, v_y) + S(v_x, v_y)|^2}{1 + m/(\lambda f_l)^2 |R(v_x, v_y) + S(v_x, v_y)|^2 \exp(-\Gamma l)} \right]^{1/2} \quad (1)$$

where v_x and v_y are spatial frequencies, m is the beam intensity ratio before passage of the signal beam through the transparency bearing the objects $g = |r + s|$, λ is the wavelength, f_l is the focal length, and R and S are the Fourier spectra of r and s , respectively.

For low coupling equation 1 can be approximated as

$$A(v_x, v_y) = A(0) - (\Gamma l) \frac{m/(\lambda f_l)^2 |R(v_x, v_y) + S(v_x, v_y)|^2}{1 + m/(\lambda f_l)^2 |R(v_x, v_y) + S(v_x, v_y)|^2} \quad (2)$$

The magnitudes of the functions r and s are between 0 and 1, since they represent the transmittance function of the object. The quadratic term in Eq. (1) is responsible for mixing the Fourier transforms R and S , thereby producing the appropriate signal processor functionality such as correlation or convolution.

An important factor that can affect the correlation peak-intensity is the grating efficiency of energy transfer in two beam coupling:

$$\eta_t(z) = \frac{|A_2(z)|^2}{|A_1(0)|^2} = \sin^2[u(m, \Gamma z)] \quad (3)$$

Where

$$u(m, \Gamma z) = \left\{ \frac{2m[1 + \cosh(m^{-1})]}{(1 + m)^2} \right\}^{1/2} \times \left[\tan^{-1} \exp\left(\frac{\Gamma z}{2} + \frac{1}{2m}\right) - \tan^{-1} \exp\left(\frac{1}{2m}\right) \right] \quad (4)$$

Figure 2(A) shows the intensity of the output beam as a function the beam ratio where the coupling coefficient was taken as a parameter and figure 2(B) is the grating efficiency as a function the beam ratio. The plots are based on equation 1.

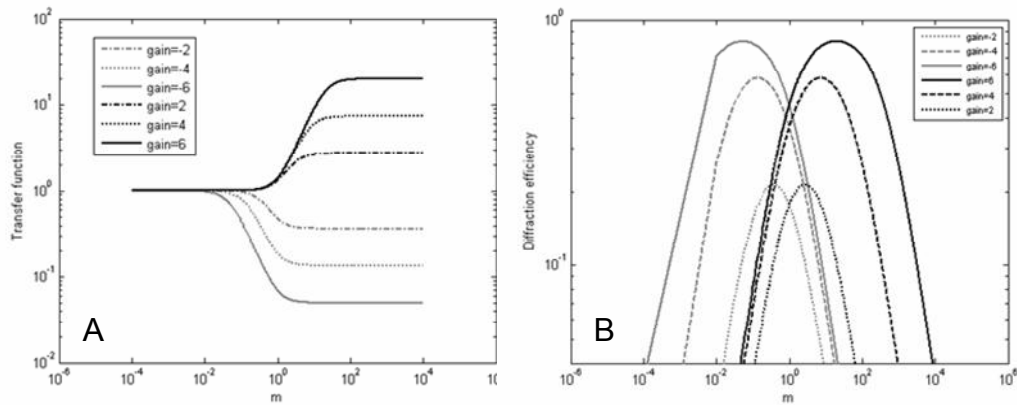


Figure 2. (A) The intensity of the output beam as a function the beam ratio for different coupling coefficients, (B) the grating efficiency as a function of beam ratio for different coupling coefficients.

4. SCATTERING CENTER ENHANCEMENT & DYNAMIC RANGE COMPRESSION

Figure 3 shows the computer simulation on scattering center enhancement.

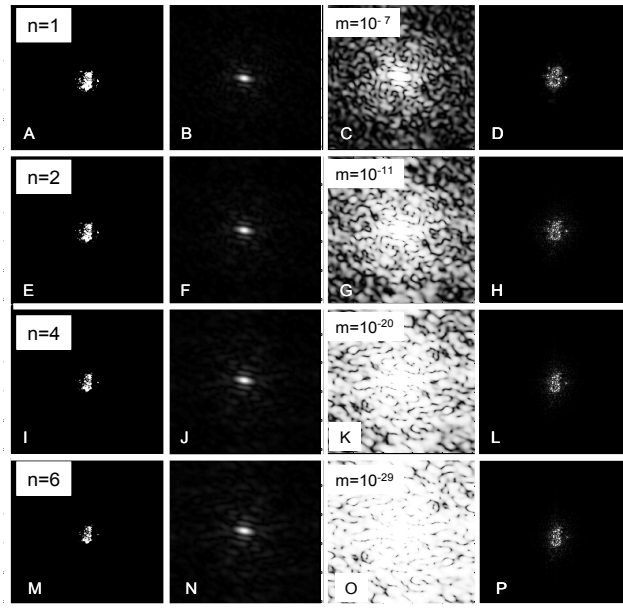


Figure 3. The first column power-law enhanced scattering images of the SAR image HB03333 extracted from the ROI (MSTAR/15-DEG/COL1/SCENE1/BTR-60). The respective power-law enhancements for the first column are “1”, “2”, “4” and “6”. The second column is their respective Fourier transforms. The third column is their dynamic range compressed Fourier transforms with different beam compression values. The beam ratios for C, G, K and O respectively are $m=10^{-7}$, $m=10^{-11}$, $m=10^{-20}$ and $m=10^{-29}$. The last column is the respective enhanced scattering center images after applying dynamic range compression, with a beam ratio of 10^{-7} on the Fourier spectra in the second column.

Figure 3A shows an example of a gray-level SAR image (MSTAR/15-DEG/COL1/SCENE1/BTR-60/HB03333) extracted from the ROI. The small bright spots in the image are termed the scattering centers. These centers are related to the shape of the target and are independent of target translation. Its Fourier transform, as shown in Fig. 3B, consists of mostly a dc peak with very little information at the neighboring low frequencies. It is difficult to use such information for direct target recognition because there is too little edge information that even applying edge-enhancement algorithms wouldn't help. Therefore a correlation system using this kind of information will suffer from many false alarms and very low probability of detection. There are three techniques for enhancing the scattering centers of a SAR image: (1) applying a pure dynamic range compression on the image's Fourier spectrum, (2) raising the image to a certain power, and (3) applying both the dynamic range compression and the power-law enhancement simultaneously. Figure 3C shows the effect of dynamic range compression implementation on the Fourier spectrum, shown in Fig. 3B, according to modified version of two-beam coupling nonlinear energy transfer as discussed in equations 1 and 2. As one see in figure 3C the high frequencies are significantly enhanced compared to the low frequencies. The dynamic range compression effectively leads to a significant enhancement of the scattering centers, which is demonstrated in Fig. 3D (the inverse Fourier transform of the compressed spectrum presented in Fig. 3C). The results of applying the second approach (i.e. enhancing the scattering centers using the power-law) are shown in Figs 3E, 3I and 3M. They are the enhanced scattering centers of the image as the power increases by $n=2$, 4 and 6 respectively. It is clear that there is significant enhancement of high frequencies relative to the low frequencies as the power increases. Further enhancement in high frequencies can be achieved by applying the dynamic range compression. Figures 3G, 3K and 3O show the results of applying the modified two-beam coupling dynamic range compression on the Fourier spectra shown in Figs 3F, 3J, and 3D respectively. The beam ratios for dynamic range compression have been reduced as the power increased. The respective beam ratios are 10^{-7} , 10^{-11} , 10^{-20} and 10^{-29} . Figures 3H, 3L and 3P show respectively the inverse Fourier transforms of the compressed Fourier spectra shown in Figs 3G, 3K and 3O. As a general concluding remark from these results, either increasing the power or implementing the dynamic range compression leads to enhancing the scattering centers.

However, the enhancement in the images scattering centers was more prominent when dynamic range compression was implemented. This can be verified by comparing figures 3D and 3M. The combination between power-law enhancement and dynamic range compression did not lead to significant enhancement in the scattering center compared to implementing dynamic range compression.

Although the combination of power-law and dynamic range compression did not lead to any significant advantage over just implementing dynamic range compression for enhancement of the scattering centers; however, their combination is more effective in removing the clutter surrounding the target. This is shown in Figure 4. We set the 128x128 SAR images within 256x256 zeros arrays. The images were raised to a certain power and then Fourier transformed. The Fourier transform data was terminated via a 128x128 window and then the two-beam coupling dynamic range compression was applied on the spectrum. The first column respectively is the results of applying power-law enhancement for the powers of 1, 2, 4, 6, while the second column respectively are the results of implementation of the above procedure. Applying power-law enhancement showed not only an enhancement in the scattering center, but also improved the signal-to-clutter. Implementation of dynamic range compression with low pass filtering alone without power-law enhancement as shown in the first row (Figures 4A and 4A') produced some enhancement in the target's scattering centers and signal-to-clutter ratio. The enhancement of the scattering centers due to solely dynamic range compression implementation (Fig 4A') was always better than that due solely to power-law enhancement (Fig 4B, 4C and 4D) while the signal-to-clutter ratio was in the opposite way. However, when the power-law and the dynamic range compression enhancements were applied simultaneously, both of the scattering centers and the signal-to-clutter ratio improves as the power-law enhancement increases, which is evident by comparing the results in figures 4D', 4A' and 4D'. The results in figure 4 shows what could effectively happen to the input impulse response on clutter reduction and scattering centers enhancement for both of the matching template and the input target if the nonlinear processor is replaced by a linear processor.

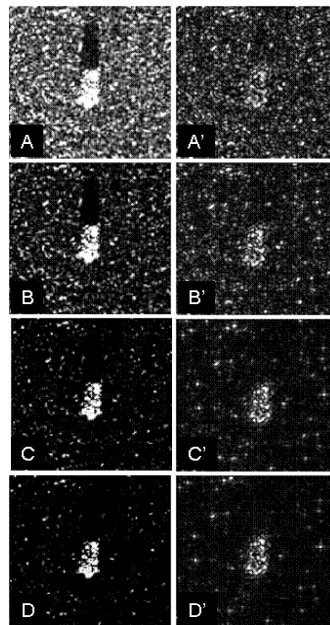


Figure 4. Enhanced SAR image, the first column is power-law enhancement of d images with respective power-law of "1", "2", "4" and "6". The second column respectively the simultaneous application of two-beam coupling dynamic range at beam ratio $m=10^{-7}$ and the respective power-law enhancements as in the first column.

It was indicated above that applying dynamic range compression in an image Fourier spectrum has three effects: (1) Enhances the signal to noise ratio where the signal is lower than the noise, (2) Increases the noise frequencies which consequently leads for spreading the noise over a larger area in the spatial domain, (3) Enhances the intensity of the high frequencies compared to the low frequencies. These three effects demonstrate that dynamic range compression in the Fourier domain significantly improves the signal to noise ratio and is more effective than conventional dynamic range compression (dynamic range compression in the image domain). Applying power-law scattering center enhancement has two effects: (1) Enhances the target's high frequencies relative to its lower frequencies, (2) Increases the clutter's frequencies so that it spreads over a large area in the spatial domain. Although power-law enhancement of the scattering center is an expansion process that leads to a signal to noise reduction; however it is not applied to SAR images since the clutter is disjoint of the target. The advantages of using this procedure (i.e. the power-law enhancement) are that it: (a) enhances the signal-to-clutter Fourier spectrum energy which facilitate the preconditions for further enhancement in the signal to noise ratio through applying dynamic range compression on the Fourier spectrum and (b) converts the clutter to very high spatial frequencies, the major part of which can be blocked or filtered out with little loss in the scattering centers spectrum.

For simulating and evaluating the two-beam coupling JTC performance in SAR image recognition, a zeros array of 512x1024 consisted of a reference and a signal image selected from MSTAR database for the target, was used as the joint input. The reference target image consisted of a ROI linear superposition power-law enhanced scattered center of 5 images templates (MSTAR/15-DEG/COL1/SCENE1/BTR-60/HB03333, HB03334, HB03335, HB03337, and HB03338). The signal image is also raised to the same power. Both extended and non-extended operational conditions were simulated. In the extended simulation, the HB03341 target was selected as a signal image from the same database. In the non-extended simulation, the HB03333 target was selected as a signal image.

Figure 5 shows the joint image of the power-law enhanced scattering center linearly superimposed template and a signal image. The scattering centers of both the reference and the signal were enhanced through rising up the images to the power "n". Figures 5 (A, B, C and D) are for n equal to 1, 2, 4 and 6 respectively.

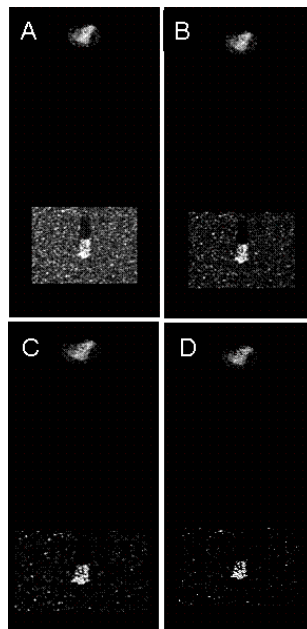


Figure 5. Joint image of power-law enhanced SAR image and syntactic template extracted from ROI. The power-law enhancement from A to D are "1", "2", "4" and "6" respectively.

The correlation results are shown in Figures 6 for beam ratio $m=10^{-7}$. Figures 6 (A, B, C and D) demonstrate the correlation peaks for scattering centers power-law enhancement through $n=1, 2, 4$ and 6 respectively. As the power increases, the correlation peak accentuates and the surrounding noise decreases.

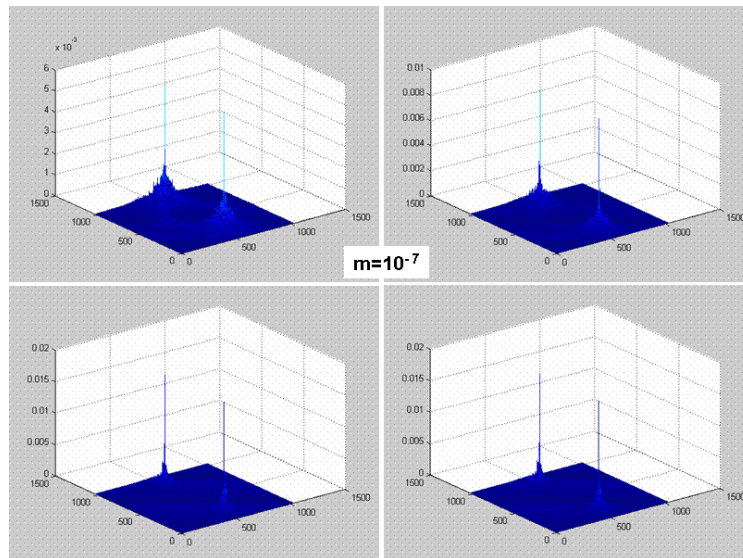


Figure 6. The two-beam coupling joint transform correlation results of the inputs in figure 3 at beam ratio of $m=10^{-7}$

For testing under extended operating conditions, we selected one image from the same target but not included in the template (in class) and one image from a different target (out of class). Figures 7 A and B show the correlation results for enhanced power-law scattering centers for $n=6$ where (A) is the in class and (B) is the out of class correlation results. By comparing figures 7(A) and 7(B) we can conclude that a distinct correlation peak appears when the target signal is in class, while noise appears when the target signal is out-of-class.

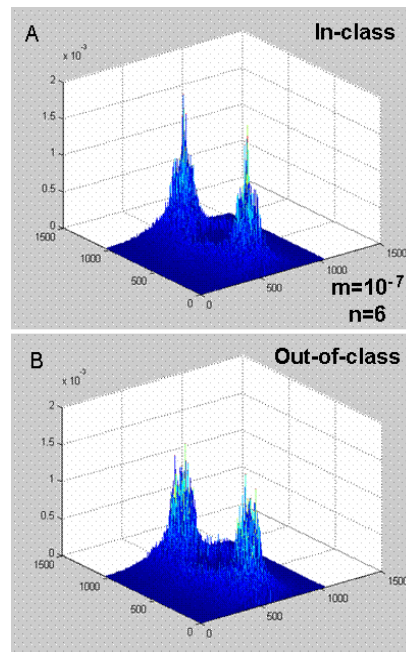


Figure 7. Joint transform correlation results with power-law enhancement of “6” and dynamic range compression for beam ratio $m=10^{-7}$ (a) For in-class target (MSTAR/15-DEG/COL1/SCENE1/BTR-60/HB03341) (b) For out-of class target (MSTAR/45_DEG/COL2/SCENE1/2S1/HB16946).

Figure 8 shows plots of (A) correlation peak-intensity, (B) peak-to-correlation energy (PCE), (C) the Horner efficiency as a function of the beam ratio where the scattering center power law enhancement of the in both the input template was selected as a parameter, (A') the correlation-peak intensity, (B') the PCE, and (C') the Horner efficiency as a function of scattering centers power-law enhancement where the beam ratios are taken as parameters. It is shown in figure 8(A) that the correlation-peak is higher as the power-law scattering center enhancement increases. This is attributed to the fact that scattering centers enhancement leads to high frequencies enhancement relative to the low frequencies which leads the correlation to focus more energy to a point. The correlation-peak increases up to a point that attributes to the dynamic range compression flattening the Fourier spectrum, and hence generating a sharp correlation peak. However, after a certain beam ratio the diffraction efficiency decreases which consequently leads to decrease in the correlation peak intensity as the beam ratio increases. The same is applied to the PCE plots, the higher the power-law scattering center enhancement the more the peak-to-correlation energy enhances. In most SAR images, the noise spectrum has higher energy than the image spectrum. Therefore, the possibility of the noise to be compressed and to be turned to a salt and pepper noise is most likely happens before the image spectrum is compressed. The correlation energy distribution relative to the grating efficiency, which mostly is from noise, remains nearly flat, while the correlation peak intensity follows, as has been plotted above. This explains the behavior similarity in PCE to that of the I_p . The behavior of the Horner efficiency is very similar to that of the correlation peak intensity as well as the peak to correlation energy. The similarity in the same behavior can be attributed to the same reasons discussed for the above curves. As concluding remarks from all of these plots, the higher power-law scattering centers enhancement leads to higher performance for all the above metrics. The power-law enhancement of the scattering center facilitates the pre-conditions for achieving dynamic range compression. The best performance for all the above metrics was for intermediate beam ratios, while the metrics values dropped down for high and low beam ratios in agreement with the plots in the prior figures.

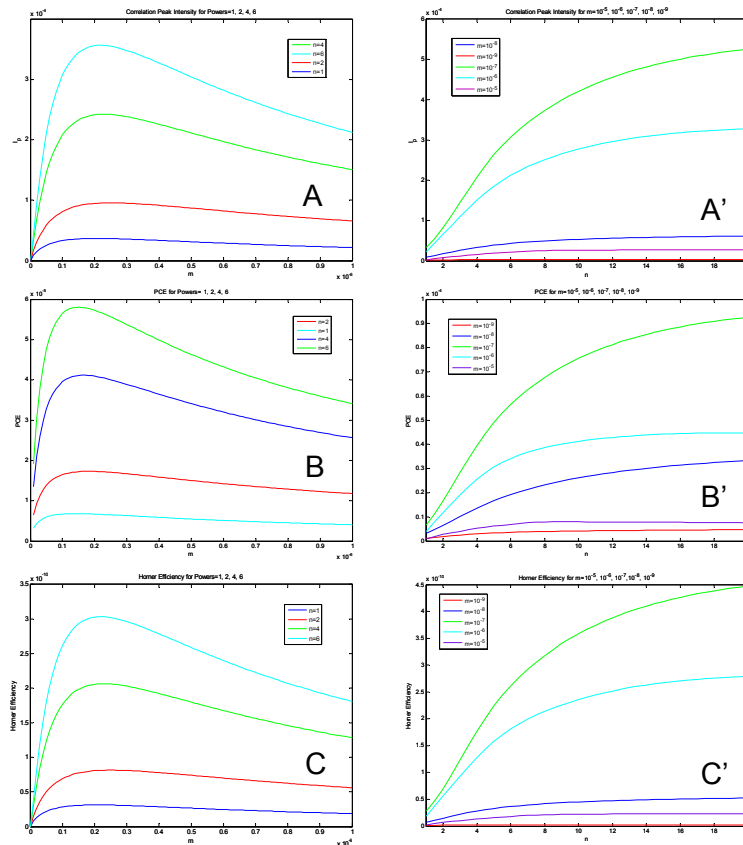


Figure 8. Plots of (A) correlation peak-intensity, I_p (B) peak- to-correlation energy PCE (C) the Horner efficiency as a function of the beam-ratio for power-law enhancement of light blue, green, red and blue. (A') correlation peak-intensity I_p (B') peak- to-correlation energy PCE and (C') the Horner efficiency versus the power law enhancement where the beam ratio has been taken as a parameter. The respective beam-ratio parameters for red, blue, green, light blue and pink are 10^{-9} , 10^{-8} , 10^{-7} , 10^{-6} and 10^{-5} .

5. CONCLUSION

In this paper we introduced Two-Beam Coupling Joint transform Correlation Synthetic Aperture Radar (SAR) Image Recognition with Power-Law Scattering Center Pre-enhancement. The SAR images were selected from Moving and Stationary Target Acquisitions and Recognition (MSTAR) database

In the computer simulation, the joint input image consists of a power-law scattering center pre-enhancement of the input image, and a linearly synthesized power-law enhanced scattering center template.

The power-law enhancement of the scattering center facilitates the preconditions (a) for less severe requirement to achieve dynamic range compression for enhancing the signal-to noise ratio (b) for blocking the noise with a small loss in the scattering centers' spectrum due to the conversion of the noise, resulting in a very high spatial frequency.

Dynamic range compression provides the following capabilities: 1) enhances signal to noise ratio; 2) enhances high frequencies relative to low frequencies; and 3) converts the noise into higher frequency components. This significantly improves the ratio of the correlation peak intensity to the mean of the surrounding noise.

It was demonstrated that the power-law per-enhancement of scattering centers accompanied with dynamic range compression, enhances the image scattering centers, and reduces the image clutter as the power increases. This subsequently leads to further enhancement in the correlation peak intensity, the peak to correlation energy and the Horner efficiency.

REFERENCES

1. B. G. Boone, *Signal Processing Using Optics: Fundamentals, Devices, Architecture and Applications* (Oxford U. Press, Oxford, 1998), Chap. 11, pp. 281–311.
2. R. Shenoy and D. P. Casasent, "Multiclass SAR feature space trajectory FST neural net class and pose estimation results", *Proc. SPIE* 3070, 121 (1997).
3. R. Murenzi, D. Semwogerere, D. Johnson, L. M. Kaplan, and K. R. Namuduri, "Detection/recognition of targets in low-resolution FLIR images using 2D directional wavelets," *SPIE Automatic Target Recognition VIII AeroSense conference* (1998).
4. S. A. Stanhope, E. Keydel, W. Williams, V. Rajilic, and R. Sieron, "The use of the mean squared error matching metric in a model based automatic target recognition system," *Proc. SPIE* 3370, 360–368 (1998).
5. M. Boshra and B. Bhanu, "Performance modeling of feature-based classification in SAR imagery," *Proc. SPIE, Algorithms for Synthetic Aperture Radar Imagery V*, Vol. 3370, pp. 661–674 (1998).
6. D. K. Barton, *Modern Radar Systems Analysis* (Artech House, Norwood, Mass., 1988), p. 209.
7. H. Urkowitz, in *Modern Radar Analysis Evaluation and System Design*, R. S. Berkowitz, ed. (Wiley, New York, 1965), Chap. 1, pp. 197–215.
8. J. Khoury, P. D. Gianino, and C. L. Woods, "Synthetic aperture radar image correlation by use of preprocessing for enhancement of scattering centers," *Opt. Lett.* 25, 1544–1546 (2000)
9. J. Khoury, Peter D. Gianino, and Charles L. Woods "Optimal synthetic aperture radar image correlation using enhanced scattering centers in holographic data storage," *Optical Engineering Volume 40, Issue 11*, pp. 2624–2637 (2001)
10. J. L. Horner and P. D. Gianino, "Phase-only matched filtering," *Appl. Opt.* 23, 812 (1984).
11. J. L. Horner and J. R. Leger, "Pattern recognition with binary phase-only filters," *Appl. Opt.* 24, 609–611 (1985).
12. J. Khoury, J. Fu, M. Cronin-Golomb, and C. Woods, "Quadratic processing and nonlinear optical phase rectification in noise reduction," *J. Opt. Soc. Am. B* 11, 1960– (1994)
13. J. Khoury, M. Cronin-Golomb, P. Gianino, and C. Woods, "Photorefractive two-beam coupling nonlinear joint transform correlator," *J. Opt. Soc. Am. B* 11, 2167– (1994)
14. G. Asimellis, J. Khoury, and C. Woods, "Effects of saturation on the nonlinear incoherent-erasure joint-transform correlator," *J. Opt. Soc. Am. A* 13, 1345– (1996)
15. J. Khoury, George Asimellis Peter D. Gianino and Charles L. Woods "Nonlinear compansive noise reduction in joint transform correlators," *Optical Engineering Optical Engineering* 37(01), pp.66–74 (1998)
16. Mohammad S. Alam , Jehad S. Khoury "Fringe-adjusted incoherent erasure joint transform correlator," *Optical Engineering* 37(01), pp.75–82 (1998)
17. Bahareh Haji-saeed; Sandip K. Sengupta; William D. Goodhue; Jed Khoury; Charles L. Woods; John Kierstead "Dynamic range compression deconvolution using A-law and μ -law algorithms," *Proceedings Vol. 6574 Optical Pattern Recognition XVIII* (2007)
18. B. Haji-saeed, S. K. Sengupta, W. Goodhue, J. Khoury, C. L. Woods, and J. Kierstead, "Nonlinear dynamic range compression deconvolution," *Opt. Lett.* 31, 1969–1971 (2006)
19. B. Haji-saeed, W. D. Goodhue, J. Khoury, C. L. Woods, and J. Kierstead, " Dynamic Range Compression Deconvolution," in *Frontiers in Optics* (2007)
20. D. Casasent and S. Ashizawa, "Synthetic aperture radar detection, recognition and clutter rejection with minimum noise and correlation energy filters," *Opt. Eng.* 36, 2729–2736 (1997).
21. R. Shenoy and D. Casasent, "Eigen-MINACE detection filter with improved capacity," *Proc. SPIE* 3370, 435–447 (1998).
22. John G. Proakis, Masoud Salehi, "Communication Systems Engineering," Prentice Hall (2002)
23. W. B. Davenport and W. L. Root, "An Introduction to the Theory of Random Signal and Noise," ch. 12–13, p. 255–311, McGraw-Hill, New York (1958)
24. Rafael C. Gonzalez, Richard E. Woods, "Digital Image Processing," Prentice Hall (2002)
25. <http://hyperphysics.phy-astr.gsu.edu/hbase/audio/tape4.html#c2>